Indirect Adaptive Robust Control of Hydraulic Manipulators With Accurate Parameter Estimates

Amit Mohanty, *Student Member, IEEE*, and Bin Yao, *Senior Member, IEEE*

***Abstract*—In a general direct adaptive robust control (DARC) framework, the emphasis is always on the guaranteed transient performance and accurate trajectory tracking in presence of *uncertain nonlinearities* and *parametric uncertainties*. Such a direct algorithm suffers from lack of modularity, controller-estimator inseparability, and poor convergence of parameter estimates. In the DARC design the parameters are estimated by gradient law with the sole purpose of reducing tracking error, which is typical of a Lyapunov-type design. However, when the controller-estimator module is expected to assist in secondary purposes such as health monitoring and fault detection, the requirement of having accurate online parameter estimates is as important as the need for the smaller tracking error. In this paper, we consider the trajectory tracking of a robotic manipulator driven by electro-hydraulic actuators. The controller is constructed based on the indirect adaptive robust control (IARC) framework with necessary design modifications required to accommodate uncertain and nonsmooth nonlinearities of the hydraulic system. The online parameter estimates are obtained through a parameter adaptation algorithm that is based on physical plant dynamics rather than the tracking error dynamics. While the new controller preserves the nice properties of the DARC design such as prescribed output tracking transient performance and final tracking accuracy, more accurate parameter estimates are obtained for prognosis and diagnosis purpose. Comparative experimental results are presented to show the effectiveness of the proposed algorithm.**

***Index Terms*—Adaptive control, hydraulic system, parameter estimation, robust control.**

I. Introduction

HYDRAULIC systems have been widely used in industry where large actuation forces are needed. Examples include electro-hydraulic positioning system [1], active suspension control [2], and industrial hydraulic machine [3]. Industrial use of hydraulic actuation presents a unique challenge from a controls point of view. The nontriviality of the control problem arises from many sources, such as nonsmooth nonlinearities present in the pressure dynamics, presence of deadbands in valve operation, unmodeled friction, control saturation, etc. Apart from nonlinearity of the system, there also exists model uncertainties due to idealization of a physical process by a mathematical model. We classify all those uncertainties into two classes: *parametric uncertainties* and *uncertain nonlinearities*. Parametric uncertainties arise due to lack of knowledge of various physical parameters of the system, e.g., the payload lifted by an industrial hydraulic manipulator, change in the bulk modulus of the hydraulic fluid due to change in temperature or introduction of foreign particles. We can not employ offline system identification techniques to estimate them, as those offline estimated nominal parametric values may change over the time or even during the control action. There is another class of uncertainty, which can not be modeled exactly and the nonlinear functions that describe them are unknown, e.g., inexact friction model, leakage in the hydraulic circuit. Those type of uncertainties are classified as *uncertain nonlinearity*.

Linear control theory [1], [4]–[6] and feedback linearization techniques [7] have been widely used for the control of hydraulic systems. However, linear techniques are fundamentally incapable of achieving high performance for the control of a hydraulic system [8]. In [9], the direct adaptive robust control (DARC) technique proposed by Yao and Tomizuka in [10], [11], [20], and [21] was applied to precision motion control of electro-hydraulic systems driven by single-rod actuators. However, being a direct Lyapunov-based design method, it does not provide the freedom to choose the parameter estimation law independent of the controller design. The intertwining design of the controller and the estimation module, whose sole objective is to reduce the output tracking error, forces us to use gradient-type estimation law. It is well known that the gradient type of parameter estimation law may not have as good convergence properties as other types of estimation laws (e.g., the least squares method). The DARC algorithm uses actual tracking errors as driving signals for parameter estimation. Although the desired trajectory might be persistently exciting (PE), the actual tracking errors in implementation are normally very small and thus, the parameter adaptation is prone to be corrupted by other neglected factors such as sampling delay and noise. As a result, in implementation, the parameter estimates are not accurate enough to be used for secondary purposes, e.g., prognosis and machine component health monitoring. To overcome the poor parameter estimation properties of the DARC design [11], an indirect adaptive robust control (IARC) design for single-input-single-output (SISO) nonlinear systems with parametric semi-strict feedback form has recently been proposed [12].

This paper focuses on the precision motion control of an electro-hydraulic robotic arm driven by single-rod hydraulic

Manuscript received November 21, 2008; revised June 02, 2009 and December 06, 2009; accepted December 14, 2009. Manuscript received in final form April 13, 2010. First published May 24, 2010; current version published April 15, 2011. Recommended by Associate Editor R. Landers. This work was supported in part by the National Science Foundation under Grant CMS-0600516.

A. Mohanty is with the Ray W. Herrick Laboratory, School of Mechanical Engineering, Purdue University, West Lafayette, IN 47907 USA (e-mail: amitmohanty@gmail.com).

B. Yao is with the Ray W. Herrick Laboratory, School of Mechanical Engineering, Purdue University, West Lafayette, IN 47907 USA, and also with the State Key Laboratory of Fluid Power Transmission and Control, Zhejiang University, Hangzhou 310027, China (e-mail: byao@purdue.edu).

Color versions of one or more of the figures in this paper are available online at http://ieeexplore.ieee.org.

Digital Object Identifier 10.1109/TCST.2010.2048569

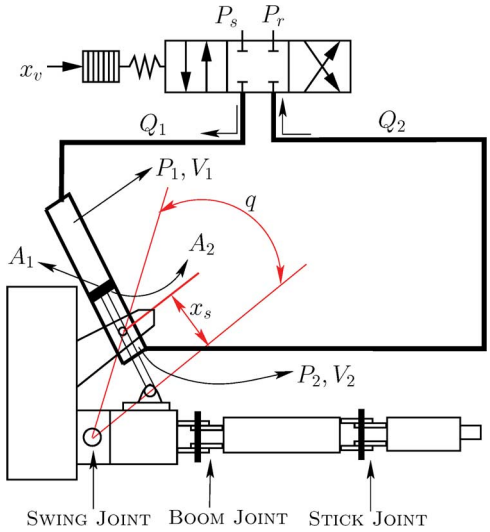

Fig. 1. Robotic manipulator with hydraulic actuation.

actuator in the IARC framework as proposed in [12]. The modeling and problem formulation was carefully done in Section II, so that in spite of the presence of nonsmooth nonlinearities such as pressure dynamics and terms like Columbic friction, the IARC algorithm can be applied to the hydraulic system. In Section III, the controller is designed to overcome the poor parameter estimation problem of the DARC designs without sacrificing the guaranteed transient performance of the DARC design. This was achieved by separating the construction of parameter estimation law from the design of underlying robust control law using nonlinear X-swapping-based techniques. In Section III-D, it was shown that a guaranteed transient performance and final tracking accuracy for output tracking can be achieved even in the presence of disturbances and uncertain nonlinearities. In Section IV, we present comparative experimental results to verify the effectiveness of the proposed controller.

II. Dynamic Model and Problem Formulation

In this paper, we consider a three degrees-of-freedom (DOF) hydraulic robot arm shown in Fig. 1. To make the idea easy to understand, only the swing joint motion is considered while the other two joints (boom and stick) are kept fixed. As shown in [9], the dynamics of the swing motion can be described by

$$J\ddot{q} = \left(\frac{\partial x_s}{\partial q}\right)(P_1A_1 - P_2A_2) - B\cdot\dot{q} - A\cdot\mathcal{S}(\dot{q}) + D_{1n} + \widetilde{D}_1 \quad (1)$$

where J is the moment of inertia of the robotic arm and external payload lumped together, q is the angular displacement of the swing joint, $\partial x_s/\partial q$ is the first-order partial derivative of cylinder displacement x_s with respect to the swing angle q, P_1, and P_2 are the pressures in the cylinder forward and return chamber, respectively, A_1 and A_2 are the ram areas of the forward and return chambers, respectively, B represents the combined damping and viscous friction coefficient, A represents the magnitude of modeled Coulomb friction force, $\mathcal{S}(\bullet)$ represents the usual signum function, and $(D_{1n} + \widetilde{D}_1)$ is the lumped modeling error including external disturbances and terms like the unmodeled friction forces and uncertainties, in which D_{1n} represents its nominal value.

The supply flow Q_1 and return flow Q_2 through the servo valve used in the experiments can be modeled by [13]

$$Q_1 = k_{q1}x_v\sqrt{|\Delta P_1|}, \quad \Delta P_1 = \begin{cases} P_s - P_1, & x_v \geq 0 \\ P_1 - P_r, & x_v < 0 \end{cases} \quad (2)$$

$$Q_2 = k_{q2}x_v\sqrt{|\Delta P_2|}, \quad \Delta P_2 = \begin{cases} P_2 - P_r, & x_v \geq 0 \\ P_s - P_2, & x_v < 0 \end{cases} \quad (3)$$

where x_v is the spool displacement, k_{q1} and k_{q2} are the flow gain coefficients for the forward and return loop, respectively, P_s is the supply pressure of the pump and P_r is the reference pressure in the return tank. Ignoring the relatively much faster valve dynamics, the spool displacement x_v can be modeled as a known static mapping of control input current u. Without loss of generality, we assume the static map to be $x_v = u$ and any non-unity gain between x_v and u is taken care of by constants k_{q1} and k_{q2} as in [9]. The cylinder pressure dynamics can be written as [13]

$$\frac{V_1(q)}{\beta_e}\dot{P}_1 = -A_1\frac{\partial x_s}{\partial q}\dot{q} + Q_1 + D_{21n} + \widetilde{D}_{21} \quad (4)$$

$$\frac{V_2(q)}{\beta_e}\dot{P}_2 = +A_2\frac{\partial x_s}{\partial q}\dot{q} - Q_2 - D_{22n} - \widetilde{D}_{22} \quad (5)$$

where $V_1(q)$ and $V_2(q)$ are the total volumes of the forward and return chamber respectively, β_e is the effective bulk modulus. $D_{21n} + \widetilde{D}_{21}$ and $D_{22n} + \widetilde{D}_{22}$ are the lumped modeling error and uncertainties in the forward and return loop respectively, which can be attributed to the non-exact proportional nature of servo valves and the presence of leakages in the hydraulic circuit. D_{21n} and D_{21n} are the nominal values of these uncertainties.

In general, the system is subjected to parametric uncertainties due to lack of complete information on J, B, A, D_{1n}, D_{21n}, D_{22n}, and β_e. We define a set of the parameters as: $\theta_1 = J$, $\theta_2 = B$, $\theta_3 = A$, $\theta_4 = D_{1n}$, $\theta_5 = \beta_e^{-1}$, $\theta_6 = D_{21n}$, and $\theta_7 = D_{22n}$. The system described by (1), (4) and (5) can be expressed in the following parametric form:

$$\theta_1\ddot{q} = \frac{\partial x_s}{\partial q}(P_1A_1 - P_2A_2) - \theta_2\dot{q} - \theta_3\mathcal{S}(\dot{q}) + \theta_4 + \widetilde{D}_1 \quad (6)$$

$$\theta_5\dot{P}_1 = -\frac{A_1}{V_1}\frac{\partial x_s}{\partial q}\dot{q} + \frac{1}{V_1}Q_1 + \frac{1}{V_1}\theta_6 + \frac{1}{V_1}\widetilde{D}_{21} \quad (7)$$

$$\theta_5\dot{P}_2 = +\frac{A_2}{V_2}\frac{\partial x_s}{\partial q}\dot{q} - \frac{1}{V_2}Q_2 - \frac{1}{V_2}\theta_7 - \frac{1}{V_2}\widetilde{D}_{22}. \quad (8)$$

The following nomenclature is used throughout this paper: $\widehat{\bullet}$ is used to denote the estimate of $\bullet$, $\widetilde{\bullet}$ is used to denote the estimation error of $\bullet$, e.g., $\widetilde{\theta} = \widehat{\theta} - \theta$, $\bullet_i$ is the ith component of the vector $\bullet$, $\bullet_{\max}$, and $\bullet_{\min}$ are the maximum and minimum value of $\bullet(t)$ for all t, respectively.

Since the extents of the parametric uncertainties and uncertain nonlinearities are normally known, the following practical assumptions are made.

Assumption 1: The unknown parameter vector θ lies within a known bounded convex set Ω_θ. Without loss of generality, it is assumed that $\theta_{i\min} \leq \theta_i \leq \theta_{i\max}$, $i = 1, \ldots, 7$, where $\theta_{i\min}$ and $\theta_{i\max}$ are some known constants.

Assumption 2: All the uncertain nonlinearities are bounded, i.e., $\widetilde{D}_i \in \Omega_d \triangleq \{D_i : |D_i| \leq \delta_i, i = 1, 21, 22\}$, where $\delta_i(t)$ is a known bounded function.

Let $q_d(t)$ be the reference motion trajectory, which is assumed to be bounded with bounded derivatives up to the third order. *Given the desired motion trajectory $q_{d(t)}$, the control objective* follows:

1) is to synthesize a control input u such that the output q tracks q_d as closely as possible;
2) to design a parameter estimation algorithm such that reasonably accurate parameter estimates can be obtained, in spite of various model uncertainties.

III. Indirect Adaptive Robust Controller Design

In this section, an IARC scheme will be developed for the system (6)–(8). As in [12], the first step is to use a rate-limited projection type adaptation law structure to achieve a controlled learning or adaptation process.

A. Projection Type Adaption Law Structure With Rate Limits

One of the key elements of the IARC design is to use the practical available *a prior* information to construct the projection type adaptation law for a controlled learning process. As in [11] and [14], we will use the following projection mapping $Proj_{\hat{\theta}}(\bullet)$ [15], [16] to always keep the parameter estimates within the known bounded set Ω_θ

$$\mathrm{Proj}_{\hat{\theta}}(\zeta) = \begin{cases} \zeta, & \widehat{\theta} \in \overline{\Omega}_\theta \text{ or } n_{\hat{\theta}}^T \zeta \leq 0 \\ \left(I - \Gamma \frac{n_{\hat{\theta}} n_{\hat{\theta}}^T}{n_{\hat{\theta}}^T \Gamma n_{\hat{\theta}}} \right) \zeta, & \widehat{\theta} \in \partial\Omega_\theta \ \& \ n_{\hat{\theta}}^T \zeta > 0 \end{cases} \tag{9}$$

where $\zeta \in R^p$, $\Gamma(t) \in R^{p \times p}$ is any time-varying positive definite symmetric matrix, $\overline{\Omega}_\theta$ and $\partial\Omega_\theta$ denote the interior and the boundary of Ω_θ, respectively, and $n_{\hat{\theta}}$ represents the outward unit normal vector at $\widehat{\theta} \in \partial\Omega_\theta$.

In order to achieve a complete separation of estimator design and robust control law design, in addition to the projection type parameter adaptation law (9), it is also necessary to use the preset adaptation rate limits for a controlled estimation rocess. For this purpose, define a saturation function as

$$\mathrm{sat}_{\dot{\theta}_M}(\zeta) = s_0 \zeta, \quad s_0 = \begin{cases} 1, & \|\zeta\| \leq \dot{\theta}_M \\ \frac{\dot{\theta}_M}{\|\zeta\|}, & \|\zeta\| > \dot{\theta}_M \end{cases} \tag{10}$$

where $\dot{\theta}_M$ is a preset rate limit. The following lemma summarizes the structural properties of the parameter estimation algorithm to be used in this paper [12].

Lemma 1: Suppose that the parameter estimate $\widehat{\theta}$ is updated using the following projection type adaptation law and a preset adaptation rate limit $\dot{\theta}_M$:

$$\dot{\widehat{\theta}} = \mathrm{sat}_{\dot{\theta}_M}\left(\mathrm{Proj}_{\hat{\theta}}(\Gamma\tau)\right), \quad \widehat{\theta}(0) \in \Omega_\theta \tag{11}$$

where τ is the adaptation function and $\Gamma(t) > 0$ is the continuously differentiable positive symmetric adaptation rate matrix. With this adaptation law, the following desirable properties hold.

P1) The parameter estimates are always within the known bounded set Ω_θ, i.e., $\widehat{\theta}(t) \in \Omega_\theta, \forall t$. Thus, from Assumption 1, $\theta_{i\min} \leq \widehat{\theta}_i(t) \leq \theta_{i\max}, i = 1, \ldots, 7, \forall t$.

P2)

$$\widetilde{\theta}^T \left(\Gamma^{-1} \mathrm{Proj}_{\hat{\theta}}(\Gamma\tau) - \tau \right) \leq 0, \quad \forall \tau. \tag{12}$$

P3) The parameter update rate is uniformly bounded by $\|\dot{\widehat{\theta}}(t)\| \leq \dot{\theta}_M, \forall t$.

♦

B. Indirect Adaptive Robust Control Law

In a modularized backstepping design [17], the system is usually assumed to be in strict feedback form without any uncertain nonlinearities. So, the boundedness of the parameter estimates and their derivatives can be achieved through the use of estimation algorithms with normalization and/or certain nonlinear damping. But in presence of disturbances and uncertain nonlinearities, as considered in this problem, to guarantee such an assertion is not always possible. Departing from the modularized adaptive backstepping designs, in this paper, the available *a priori* knowledge on the physical bounds of unknown parameters along with preset adaptation rate limits is used to construct a projection type parameter estimation algorithm with rate limits as described by (11) for a controlled estimation process. So, regardless of the specific adaptation law to be used (the gradient method or the least squares method, with or without normalization), the parameter estimation errors and the rate of parameter adaptation are always bounded by some known values as summarized in Lemma 1. In this subsection, these properties will be fully exploited to synthesize the underlying adaptive robust control law to achieve a guaranteed transient performance and final tracking accuracy even in the presence of disturbances and uncertain nonlinearities. This is very important from an application point of view.

Let us define a set of state variables as $x = [x_1\ x_2\ x_3\ x_4]^T \triangleq [q\ \dot{q}\ P_1 A_1\ P_2 A_2]^T$. The entire system (6)–(8) can be expressed as

$$\dot{x_1} = x_2 \tag{13}$$

$$\theta_1 \dot{x}_2 = \frac{\partial x_s}{\partial q}(x_3 - x_4) - \theta_2 x_2 - \theta_3 \mathcal{S}(x_2) + \theta_4 + \widetilde{D}_1 \tag{14}$$

$$\theta_5 \dot{x}_3 = -\frac{A_1^2}{V_1}\frac{\partial x_s}{\partial q} x_2 + \theta_6 \frac{A_1}{V_1} + \frac{A_1}{V_1} Q_1 + \frac{\widetilde{D}_{21} A_1}{V_1} \tag{15}$$

$$\theta_5 \dot{x}_4 = +\frac{A_2^2}{V_1}\frac{\partial x_s}{\partial q} x_2 - \theta_7 \frac{A_2}{V_2} - \frac{A_2}{V_2} Q_2 - \frac{\widetilde{D}_{22} A_2}{V_2}. \tag{16}$$

Define a variable z_2 as

$$z_2 = \dot{z_1} + k_1 z_1 = x_2 - x_{2eq}, \quad x_{2eq} \triangleq \dot{x}_{1d} - k_1 z_1 \tag{17}$$

where $z_1 = x_1 - q_d(t)$ is the output tracking error and k_1 is any positive feedback gain. Since $G_s(s) = z_1(s)/z_2(s) = 1/(s + k_1)$ is a stable transfer function, making z_2 small or converging to zero is equivalent to making z_1 small or converging

to zero. So the rest of the design is to make z_2 as small as possible with a guaranteed transient performance. Differentiating (17) and noting (14), we get

$$\theta_1 \dot{z}_2 = \frac{\partial x_s}{\partial q}(x_3 - x_4) - \theta_2 x_2 - \theta_3 \mathcal{S}(x_2) + \theta_4 + \widetilde{D}_1 - \theta_1 \dot{x}_{2eq}. \tag{18}$$

Define the net actuator force as $F_L = x_3 - x_4$, which can be treated as the virtual control input to (18). Design a virtual control law α_2 for F_L as follows:

$$\begin{aligned}\alpha_2(x_1, x_2, \widehat{\theta}, t) &= \alpha_{2a} + \alpha_{2s} \\ &= \alpha_{2a} + \alpha_{2s1} + \alpha_{2s2} \qquad (19)\\ \alpha_{2a} &= \left(\frac{\partial x_s}{\partial q}\right)^{-1} \\ &\quad \times \left[\widehat{\theta}_1 \dot{x}_{2eq} + \widehat{\theta}_2 x_2 + \widehat{\theta}_3 \mathcal{S}(x_2) - \widehat{\theta}_4\right] \qquad (20)\\ \alpha_{2s1} &= -\left(\frac{\partial x_s}{\partial q}\right)^{-1} k_2 z_2 \qquad (21)\\ \alpha_{2s2} &= -\left(\frac{\partial x_s}{\partial q}\right)^{-1} k_{2s}(x_1, x_2, t) z_2 \qquad (22)\end{aligned}$$

where k_2 is a positive feedback gain and $k_{2s}(x_1, x_2, t)$ is a nonlinear gain chosen large enough such that following two conditions are satisfied:

$$\textbf{Condition 1.}\ z_2 \left(\frac{\partial x_s}{\partial q}\alpha_{2s2} + \widetilde{D}_1 + \varphi_2^T \widetilde{\theta}\right) \le \varepsilon_2 \tag{23}$$

$$\textbf{Condition 2.}\ z_2 \frac{\partial x_s}{\partial q}\alpha_{2s2} \le 0 \tag{24}$$

where $\varphi_2 = [\dot{x}_{2eq}\ x_2\ \mathcal{S}(x_2)\ -1\ 0\ 0\ 0]^T$ and $\varepsilon_2 > 0$ is a design parameter. The condition (23) ensures that α_{2s2} is able to attenuate uncertainties coming from both parametric uncertainty $\widetilde{\theta}$ and uncertain nonlinearity $\widetilde{D}$ to a designer-specified constant ε_2 and (24) guarantees that α_{2s2} is dissipative in nature so that it does not interfere with the functionality of the adaptation. Some detailed examples of how to choose k_{2s} such that α_{2s2} satisfies conditions 1 and 2 are given in [11] and [18].

Let $z_3 = F_L - \alpha_2$. Noting (15), (16), and (19)–(22), the following z_3 dynamics is obtained:

$$\begin{aligned}\theta_5 \dot{z}_3 = Q_L &- \left(\frac{A_1^2}{V_1} + \frac{A_2^2}{V_2}\right)\frac{\partial x_s}{\partial q}x_2 + \frac{A_1}{V_1}\theta_6 + \frac{A_2}{V_2}\theta_7 \\ &- \theta_5 \dot{\alpha}_{2c} - \theta_5 \dot{\alpha}_{2u} + \widetilde{D}_2 \qquad (25)\end{aligned}$$

where $Q_L = ((A_1/V_1)Q_1 + (A_2/V_2)Q_2)$, $\widetilde{D}_2 = ((A_1/V_1)\widetilde{D}_{21} + (A_1/V_1)\widetilde{D}_{22})$ and $\dot{\alpha}_{2c}$ and $\dot{\alpha}_{2u}$ represent the calculable and incalculable part of $\dot{\alpha}_2 = \dot{\alpha}_{2c} + \dot{\alpha}_{2u}$ as follows:

$$\dot{\alpha}_{2c} = \frac{\partial \alpha_2}{\partial x_1}x_2 + \frac{\partial \alpha_2}{\partial x_2}\widehat{\dot{x}}_2 + \frac{\partial \alpha_2}{\partial \widehat{\theta}}\widehat{\dot{\theta}} + \frac{\partial \alpha_2}{\partial t} \tag{26}$$

$$\dot{\alpha}_{2u} = \frac{\partial \alpha_2}{\partial x_2}\widetilde{\dot{x}}_2 \tag{27}$$

in which $\widehat{\dot{x}}_2$ and $\widetilde{\dot{x}}_2$ represent the estimate and the estimation error of $\dot{x}_2$ given by

$$\widehat{\dot{x}}_2 = \frac{1}{\widehat{\theta}_1}\left(\frac{\partial x_s}{\partial q}x_3 - \widehat{\theta}_2 x_2 - \widehat{\theta}_3 S_f(x_2) + \widehat{\theta}_4\right) \tag{28}$$

$$\widetilde{\dot{x}}_2 = \dot{x}_2 - \widehat{\dot{x}}_2. \tag{29}$$

Now, design a virtual control law for Q_L as

$$Q_L = Q_{La} + Q_{Ls} = Q_{La} + Q_{Ls1} + Q_{Ls2} \tag{30}$$

$$Q_{La} = \left(\frac{A_1^2}{V_1} + \frac{A_2^2}{V_2}\right)\frac{\partial x_s}{\partial q}x_2 - \frac{\partial x_s}{\partial q}z_2 + \dot{\alpha}_{2c}\widehat{\theta}_5 - \frac{A_1}{V_1}\widehat{\theta}_6 - \frac{A_2}{V_2}\widehat{\theta}_7 \tag{31}$$

$$Q_{Ls1} = -k_3 z_3 \tag{32}$$

$$Q_{Ls2} = -k_{3s}(x, t) z_3 \tag{33}$$

where k_3 is a positive feedback gain and k_{3s} is a nonlinear gain chosen large enough so that Q_{Ls2} satisfies following two inequalities:

$$\textbf{Condition 1.}\ z_3\left(Q_{Ls2} + \varphi_3^T\widetilde{\theta} - \dot{\alpha}_{2u}\theta_5 + \widetilde{D}_2\right) \le \varepsilon_3 \tag{34}$$

$$\textbf{Condition 2.}\ z_3 Q_{Ls2} \le 0 \tag{35}$$

where $\varphi_3 = [0\ 0\ 0\ 0\ \dot{\alpha}_{2c}\ -A_1/V_1\ -A_2/V_2]^T$ and $\varepsilon_3 > 0$ is a design parameter.

Finally, the control input $u = x_v$ can be solved from the following:

$$u = \frac{Q_L}{\frac{A_1}{V_1}k_{q1}\sqrt{|\Delta P_1|} + \frac{A_2}{V_2}k_{q2}\sqrt{|\Delta P_2|}}. \tag{36}$$

C. Indirect Parameter Estimation Algorithms

In a DARC framework [9], the unknown parameters for this problem would have to be defined as $\theta = [J^{-1}\ BJ^{-1}\ AJ^{-1}\ D_{1n}J^{-1}\ \beta_e\ \beta_e D_{21n}\ \beta_e D_{21n}]^T$ to accommodate both controller design and estimation algorithm. Apart from poor estimation, one of the other drawbacks for this type of design is that they are not physical plant parameters. Moreover, as the external payload θ_1 changes, other parameters, $\theta_2 - \theta_4$ also change even when the plant parameter B, A and D_n do not change. However, the indirect design has the advantage of estimating plant parameters directly as it uses the plant dynamics in the estimation model rather than the tracking error model.

The main task in this subsection is to construct a suitable parameter estimation algorithm so that improved parameter estimates can be obtained. As such, for the time being let us assume that there are no uncertain nonlinearities in the system, i.e., $\widetilde{D}_1 = \widetilde{D}_{21} = \widetilde{D}_{22} = 0$ in (6)–(8). Rewriting the system dynamics (6)–(8), one can get the following model for parameter estimation:

$$y_1 = \frac{\partial x_s}{\partial q}(x_3 - x_4) = \theta_1 \ddot{q} + \theta_2 \dot{q} + \theta_3 \mathcal{S}(\dot{q}) - \theta_4 \tag{37}$$

$$y_2 = \frac{-A_1}{V_1}\frac{\partial x_s}{\partial q}x_2 + \frac{Q_1}{V_1} = \theta_5 \dot{P}_1 - \theta_6 \frac{1}{V_1} \tag{38}$$

$$y_3 = \frac{A_2}{V_2}\frac{\partial x_s}{\partial q}x_2 - \frac{Q_2}{V_2} = \theta_5 \dot{P}_2 + \theta_7 \frac{1}{V_2}. \tag{39}$$

Let H_f be a stable low-pass filter with relative degree no less than three. Applying the filter to (37)–(39), one obtains

$$\begin{aligned} y_{1f} &= H_f\left[\frac{\partial x_s}{\partial q}(x_3 - x_4)\right] \\ &= \theta_1\ddot{q}_f + \theta_2\dot{q}_f + \theta_3\mathcal{S}(\dot{q})_f + \theta_4(-1)_f \end{aligned} \tag{40}$$

$$y_{2f} = H_f\left[\frac{-A_1\dot{x}_s + Q_1}{V_1}\right] = \theta_5 \cdot \dot{P}_{1f} - \theta_6 \cdot \left[\frac{1}{V_1}\right]_f \tag{41}$$

$$y_{3f} = H_f\left[\frac{+A_2\dot{x}_s - Q_2}{V_2}\right] = \theta_5 \cdot \dot{P}_{2f} + \theta_7 \cdot \left[\frac{1}{V_2}\right]_f \tag{42}$$

where $\ddot{q}_f$ represents the output of the filter $sH_f(s)$ for the input $\dot{q}$. The terms $\dot{q}_f$, $\mathcal{S}(\dot{q})_f$ and $(-1)_f$ represent the output of the filter $H_f(s)$ for the input $\dot{q}$, $\mathcal{S}(\dot{q})$ and (-1), respectively. Let us define a set of regressors and parameter vectors for the purpose of parameter estimation

$$\varphi_{1f} = [\ddot{q}_f\ \dot{q}_f\ \mathcal{S}(\dot{q})_f\ (-1)_f]^T,\ \theta_{1s} = [\theta_1\ \theta_2\ \theta_3\ \theta_4]^T \tag{43}$$

$$\varphi_{2f} = \left[\dot{P}_{1f},\quad -\left[\frac{1}{V_1}\right]_f\right]^T,\ \theta_{2s} = [\theta_5\quad \theta_6]^T \tag{44}$$

$$\varphi_{2f} = \left[\dot{P}_{2f},\quad +\left[\frac{1}{V_2}\right]_f\right]^T,\ \theta_{3s} = [\theta_5\quad \theta_7]^T. \tag{45}$$

A linear regression model can be obtained from (40)–(42)

$$y_{if} = \varphi_{if}^T\theta_{is},\quad i \in \{1,2,3\}. \tag{46}$$

Define the predicted output error as $\epsilon_i = \widehat{y}_{if} - y_{if}$, where $\widehat{y}_{if} = \varphi_{if}^T\widehat{\theta}_{is}$. From (46), the following prediction error model is obtained:

$$\epsilon_i = \varphi_{if}^T\widetilde{\theta}_{is},\quad i \in \{1,2,3\}. \tag{47}$$

With this static linear regression model, various estimation algorithms can be used to identify unknown parameters, among which the least squares estimation algorithm with exponential forgetting factor and covariance resetting [19] is given below. For each set of regressor and corresponding unknown parameter vectors, we can define adaptation rate matrix as follows:

$$\dot{\Gamma}_i = \alpha_i\Gamma_i - \frac{\Gamma_i\varphi_{if}\varphi_{if}^T\Gamma_i}{1 + \nu_i\varphi_{if}^T\Gamma_i\varphi_{if}},\quad \Gamma_i\left(t_r^+\right) = \rho_i I_i,\ \nu_i \geq 0 \tag{48}$$

where $\Gamma_i(0) = \Gamma_i^T(0) > 0$ and the adaptation function is defined as

$$\tau_i = \frac{1}{1 + \nu_i\varphi_{if}^T\Gamma_i\varphi_{if}}\varphi_{if}\epsilon_i,\ i = \{1,2,3\}. \tag{49}$$

In (48), $\alpha_i \geq 0$ is the forgetting factor, t_r is the covariance resetting time, i.e., the time when $\lambda_{min}(\Gamma_i(t)) = \rho_{1i}$, where ρ_{1i} is a preset lower limit for $\Gamma_i(t)$ satisfying $0 < \rho_{1i} < \rho_i$, $\lambda_{min}(\Gamma_i(t))$ is the smallest eigen value of $\Gamma_i(t)$, I_i is the identity matrix with appropriate dimension, $\nu_i \geq 0$ is the normalizing factor with $\nu_i = 0$ leading to the unnormalized algorithm. However, during real-time implementation of parameter estimation law along with forgetting factor when the regressor is not persistently exciting, $\Gamma_i(t)$ may go unbounded, i.e., $\lambda_{\max}(\Gamma_i(t)) \to \infty$ and cause estimator windup problem. To prevent this problem, the following modification is made to (48):

$$\dot{\Gamma}_i = \begin{cases} \alpha_i\Gamma_i - \frac{\Gamma_i\varphi_{if}\varphi_{if}^T\Gamma_i}{1+\nu_i\varphi_{if}^T\Gamma_i\varphi_{if}}, & \text{if } \lambda_{max}\left(\Gamma_i(t)\right) \leq \rho_M \\ & \quad \& \left\| Proj_{\widehat{\theta}}(\Gamma_i\tau_i)\right\| \leq \dot{\theta}_M \\ 0 & \text{otherwise} \end{cases} \tag{50}$$

where ρ_M is the preset upper bound for $\|\Gamma(t)\|$ with $0 < \rho_{1i} < \rho_i < \rho_M$. With this modifications, we have $\rho_{1i}I_i < \Gamma_i(t) < \rho_M I_i$. As shown in [12], we can state following lemma.

Lemma 2: When the rate-limited projection-type adaptation law (11) is used with least squares estimator (49) and (50) and prediction error calculated from (47), then $\epsilon_i \in L_2(0,\infty) \cap L_\infty[0,\infty)$ and $\dot{\widehat{\theta}} \in L_2(0,\infty) \cap L_\infty[0,\infty)$. ♦

D. Performance

Theorem 1: Under the Assumption 1 and 2, with the adaptive control law (36) and rate limited adaptation law structure (11), adaptation function (49) and adaptation rate matrix (50), all the signals in the closed-loop system are bounded and the following properties hold.

A) In general, the output tracking error has a guaranteed transient performance and a guaranteed final tracking accuracy. Furthermore, the non-negative function $V = (1/2)\theta_1 z_2^2 + (1/2)\theta_5 z_3^2$ is bounded above by

$$V \leq e^{-\lambda t}V(0) + \frac{\varepsilon}{\lambda}(1 - e^{-\lambda t}) \tag{51}$$

where $\lambda = 2 \cdot min\{k_2/\theta_1, k_3/\theta_5\}$ and $\varepsilon = \varepsilon_2 + \varepsilon_3$. ▲

B) In presence of parametric uncertainties only (i.e., $\widetilde{D}_1 = \widetilde{D}_2 = 0$), if the following persistent excitation (PE) condition is satisfied:

$$\int_t^{t+T} \varphi_{if}\varphi_{if}^T \geq \kappa_i I_p, \text{for some } \kappa_i > 0 \text{ and } T > 0 \tag{52}$$

then, in addition to results in A), the parameter converges to their true value, i.e., $\widetilde{\theta} \to 0$ as $t \to \infty$ and asymptotic tracking is also achieved, i.e., $z_1 \to 0$ as $t \to \infty$.

▲

Proof: Differentiating V while noting (18) and (25), we can obtain

$$\begin{aligned} \dot{V} =& \theta_1 z_2\dot{z}_2 + \theta_5 z_3\dot{z}_3 \\ =& z_2\left[\frac{\partial x_s}{\partial q}(z_3 + \alpha_2) - \theta_1\dot{x}_{2eq} - \theta_2 x_2 - \theta_3\mathcal{S}(x_2) + \theta_4 + \widetilde{D}_1\right] \\ &+ z_3\left[Q_L - \left(\frac{A_1^2}{V_1} + \frac{A_2^2}{V_2}\right)\frac{\partial x_s}{\partial q}\dot{x}_2 + \frac{A_1}{V_1}\theta_6 + \frac{A_2}{V_2}\theta_7 - \theta_5\dot{\alpha}_{2c}\right. \\ &\left. - \theta_5\dot{\alpha}_{2u} + \widetilde{D}_2\right]. \end{aligned} \tag{53}$$

Substituting α_2 from (19)–(22) and Q_L from (30)–(33) into (53), we can obtain

$$\begin{aligned} \dot{V} =& -k_2 z_2^2 + z_2\left(\frac{\partial x_s}{\partial q}\alpha_{2s2} + \varphi_2^T\widetilde{\theta} + \widetilde{D}_1\right) - k_3 z_3^2 \\ &+ z_3\left(Q_{Ls2} + \varphi_3^T\widetilde{\theta} - \dot{\alpha}_{2u}\theta_5 + \widetilde{D}_2\right) \\ \leq& -k_2 z_2^2 - k_3 z_3^2 + \varepsilon_2 + \varepsilon_3 \\ \leq& -\lambda \cdot V + \varepsilon \end{aligned} \tag{54}$$

which leads to (51) by using Comparison Lemma.

Now for part B, when $\widetilde{D}_1 = \widetilde{D}_2 = 0$, from part A of Theorem 1 and Lemma 2 we can show that $z_1, z_2, z_3, \widetilde{\theta}, \widehat{\theta}, \dot{\widehat{\theta}}, \varphi_{if} \in L_\infty[0,\infty)$. From (18), (25), and (47) and noting the fact that $H(s)$ is a stable low pass filter with order at least three, it is clear that $\dot{z}_2, \dot{z}_3, \dot{\epsilon}_i \in L_\infty[0,\infty)$. As $\epsilon_i \in L_2[0,\infty)$ from Lemma. 2, using Barbalat's Lemma $\epsilon_i \to 0$ as $t \to \infty$. Thus, from (47), $\varphi_{if}^T \widetilde{\theta}_{is} \to 0$ and from (49) $\tau_i \to 0$. It can be shown that the PE condition (52) guarantees the exponential convergence of parameters [16], i.e., $\widetilde{\theta} \to 0$ and $\widetilde{\theta} \in L_2[0,\infty)$. As $\widetilde{\theta} \to 0$, from (27)–(29), we get $\dot{\alpha}_{2u} \to 0$ and $\dot{\alpha}_{2u} \in L_2[0,\infty)$. Noting $\widetilde{D}_1 = \widetilde{D}_2 = 0$, we can write (54) as the following:

$$\begin{aligned}\dot{V} =& -k_2 z_2^2 - k_3 z_3^2 + z_2 \frac{\partial x_s}{\partial q}\alpha_{2s2} + z_3 Q_{Ls2} \\ &+ \left(\varphi_2^T + \varphi_3^T\right)\widetilde{\theta} + \dot{\alpha}_{2u}\theta_5 \\ \leq& -k_2 z_2^2 - k_3 z_3^2 + \varphi_2^T \widetilde{\theta} + \varphi_3^T \widetilde{\theta} + \dot{\alpha}_{2u}\theta_5. \end{aligned} \quad (55)$$

The last three terms of the right-hand side of (55) belongs to $L_2[0,\infty)$; hence, $z_2, z_3 \in L_2[0,\infty)$. From (18) and (25), it is easy to check that $\dot{z}_2$ and $\dot{z}_3$ are bounded and continuous. Using Barbalat's Lemma, we obtain $z_1, z_2, z_3 \to 0$ as $t \to \infty$. ■

Remark 1: Theorem 1 shows that under the proposed IARC algorithm, z_1, z_2 and z_3 are bounded, i.e., swing displacement x_1, swing velocity x_2 and the net actuator force $F_L = x_3 - x_4$ are bounded. However, the original system (13)–(16) has four states. Therefore, the system has an internal dynamics of degree one, which arises from the physical phenomenon that there are more than one pair of (P_1, P_2) which can produce the desired F_L. Therefore, it is important to check the stability of the internal dynamics. The experimental results obtained in this paper suggests that internal dynamics is indeed stable. A comprehensive stability analysis of internal dynamics and zero dynamics of the system is given in [9].

IV. Comparative Experimental Results

A. Experimental Setup

The schematic of the experimental setup is shown in Fig. 2. The swing circuit is driven by a single-rod cylinder (Parker D2HXTS23A with a stroke of 11 in) and controlled by a servo valve (Parker BD760AAAN10). The cylinder has a built-in LVDT sensor, which provides the position and velocity information of the cylinder movement. Pressure sensors (Omega PX603 with internal amplifier) are installed on each chamber of the cylinder. Backward difference plus filter is used to obtain the needed velocity information at high-speed movement. All analog measurement signals (the cylinder position, velocity, forward and return chamber pressures, and the supplied pressure) are fed back to a dSPACE system through a plugged-in 16-bit analog-to-digital (A/D) and digital-to-analog (D/A) board. The real-time implementation of the controller is done through the dSPACE system while a Pentium II PC is used as an user interface. The supplied pressure is 1000 lbf/in.

B. System Identification

During the experiment, a 50 lb payload was lifted by the swing arm. The corresponding combined inertia J of the swing arm and the attached payload was calculated to be 217 kg·m^2

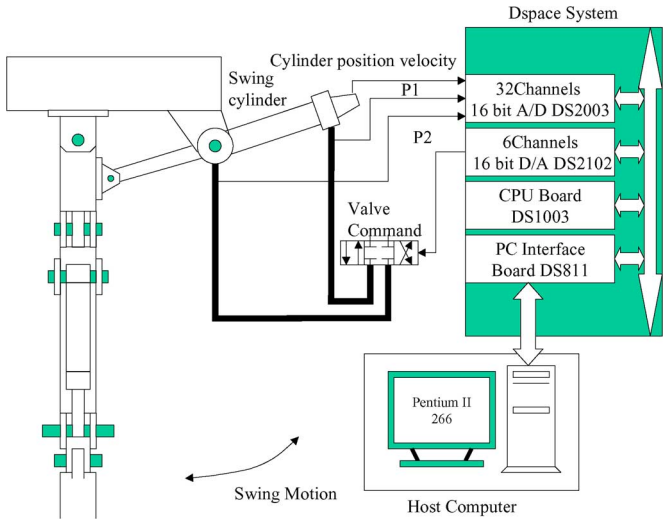

Fig. 2. Experimental setup.

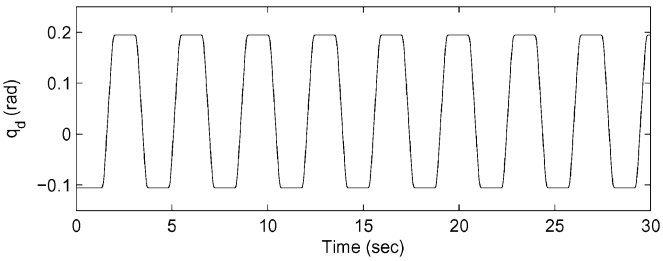

Fig. 3. Desired trajectory of swing joint.

from the geometry and material properties of the robotic arm. All the unknown parameters were estimated using system identification techniques[1] and those values were compared to parameter estimates obtained during online running of IARC. The accuracy of system identification and parameter estimation depend on various factors such as *accuracy of the model* of physical plant, *persistent excitation* level of regressors and magnitude of *uncertain nonlinearities*. Keeping these imperfections in mind, offline system identification techniques were employed using least squares algorithm to identify various unknown parameters. A pulse-type input current was fed to the servo valve and the experiment was run 20 times. The mean values of the parameter estimates were treated as the offline estimates of parameters. As the system identifications were done at different location of the swing arm working space, some variations in the offline estimated values of θ_2, θ_3, and θ_4 were observed. This indicates that the assumption of θ_2, θ_3, and θ_4 being constant over the whole working space of swing arm may not be valid. However, the same set of experiments also showed that locally θ_2, θ_3, and θ_4 appear to be constant. All the experiments in this paper were carried out keeping the joint angle in the working space $q \in [-0.1, 0.2]$ rad and thus satisfying the assumption that the unknown parameter vector θ is constant. Fig. 3 shows the desired trajectory q_d.

The offline estimated values of unknown parameter are: $\theta_1 = 217$, $\theta_2 = 14$, $\theta_3 = 30$, and $\theta_4 = 5$.

[1]In this paper, *system identification* will mean offline estimation and *parameter estimation* term would be reserved for online estimation.

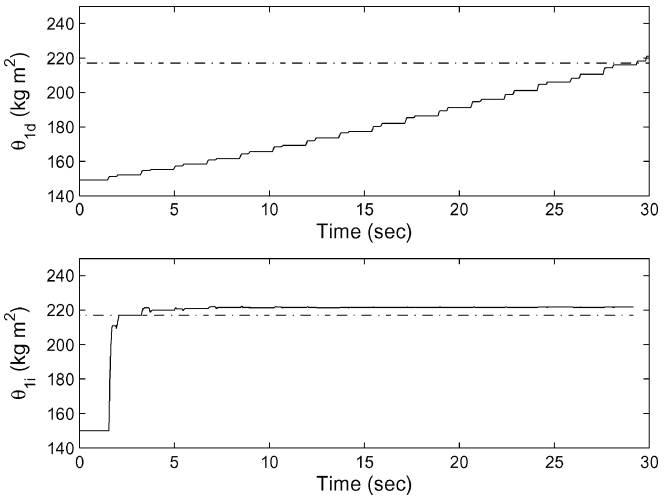

Fig. 4. Estimate of θ_1 with initial value $\widehat{\theta}_1(0) = 150$.

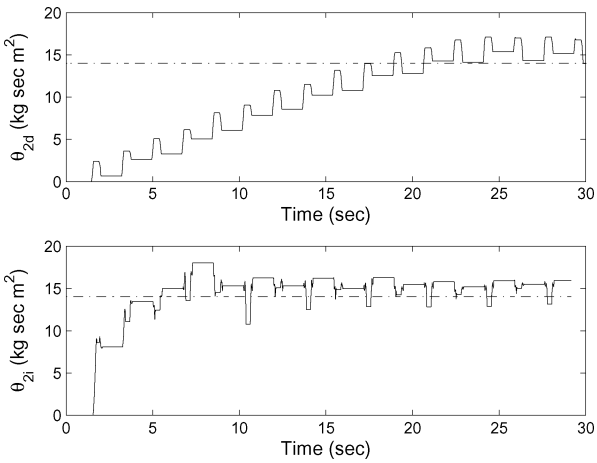

Fig. 5. Estimate of θ_2 with initial value $\widehat{\theta}_2(0) = 0$.

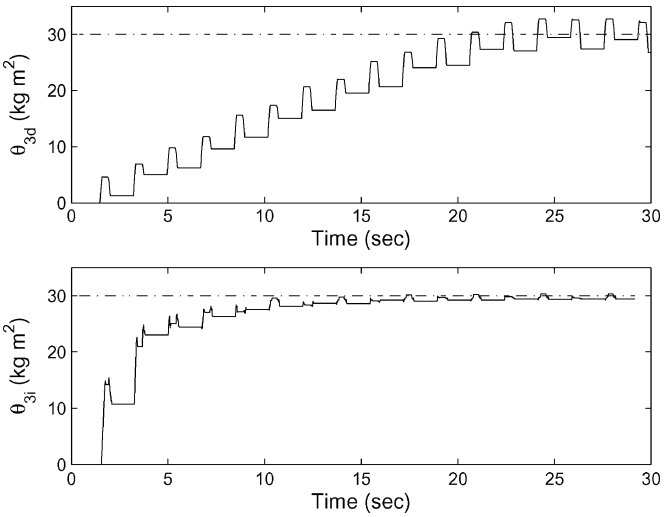

Fig. 6. Estimate of θ_3 with initial value $\widehat{\theta}_3(0) = 0$.

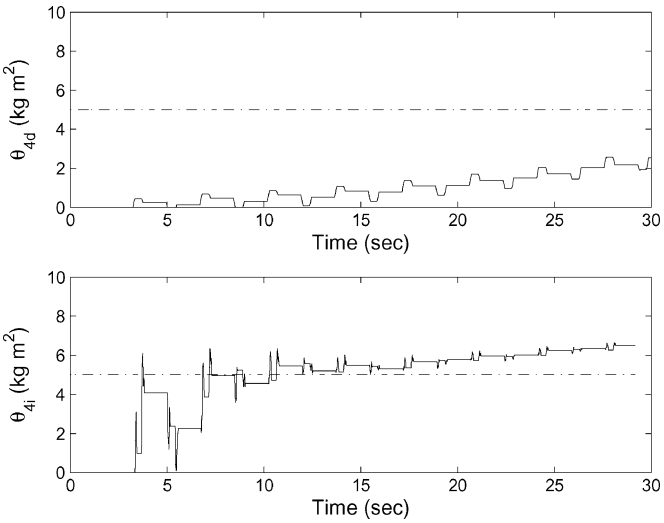

Fig. 7. Estimate of θ_4 with initial value $\widehat{\theta}_4(0) = 0$.

The cylinder physical parameters are $A_1 = 3.1416\,\text{in}^2$, $A_2 = 1.6567\,\text{in}^2$, $V_1(0) = 30.48\,\text{in}^3$, $V_2(0) = 55.33\,\text{in}^3$. The estimated flow gains are $k_{q1} = 0.1820\,\text{in}^3/(\sqrt{\text{psi}}\,\text{s V})$ and $k_{q2} = 0.1886\,\text{in}^3/(\sqrt{\text{psi}}\,\text{s V})$. The effective bulk modulus β_e is estimated to be around 2.71×10^8 Pa.

C. Controller Simplification

Some simplifications were made when implementing the proposed IARC algorithm. The solutions of k_{2s} and k_{3s} satisfying (23), (24), (34), and (35) are not unique. One set of examples of k_{2s} and k_{3s} is

$$k_{2s} \geq \frac{1}{2\varepsilon_2}\left(\|\theta_M\|^2\|\varphi_2\|^2 + \delta_1^2\right) \tag{56}$$

$$k_{3s} \geq \frac{1}{2\varepsilon_3}\left(\|\theta_M\|^2\|\varphi_3\|^2 + |\dot{\alpha}_{2u}|^2_{\max}\theta^2_{5\max} + \delta_2^2\right) \tag{57}$$

where $\theta_M = \theta_{max} - \theta_{\min}$. The selection of the specific robust control terms by (56) and (57) is formal and rigorous. However, it increases the complexity of the resulting control law considerably since it may need significant amount of computation time to calculate the exact lower bounds. A more pragmatic approach is to let $\alpha_{2s} = \alpha_{2s1} + \alpha_{2s2} = -(\partial x_s/\partial q)^{-1}K_2 z_2$ and $Q_{Ls} = Q_{Ls1} + Q_{Ls2} = -K_3 z_3$ and simply choose K_2 and K_3 large enough without worrying about the specific values of k_{2s} and k_{3s}. By doing so, (23), (24), (34), and (35) will be satisfied at least locally around the desired trajectory. The upper bound on those two gains are determined by available bandwidth of the controller. As the dynamics of the servo valve (bandwidth 8–10 Hz) was neglected during the controller design to reduce the complexity of design, the feedbacks gains were chosen to be $k_1 = 10$, $K_2 = 10$, $K_3 = 10 \times 10^{-8}$, so that the closed-loop bandwidth of the system was less than the bandwidth of the servo valve and (56) and (57) are satisfied for the given desired trajectory.

As shown in Theorem 1, the convergence of parameter estimates are guaranteed only when there is certain kind of *persistence excitation* to the system. However, the desired task trajectory may not be always persistently exciting (PE). So, ideally the parameters should be estimated only when the signal is PE. This unique ability of stopping adaptation module is provided in the proposed IARC framework. While implementing the estimators in the IARC design, the parameters are updated only when $\dot{q}_f > 0.2$ rad/s and $\ddot{q}_f > 1$ rad/s^2.

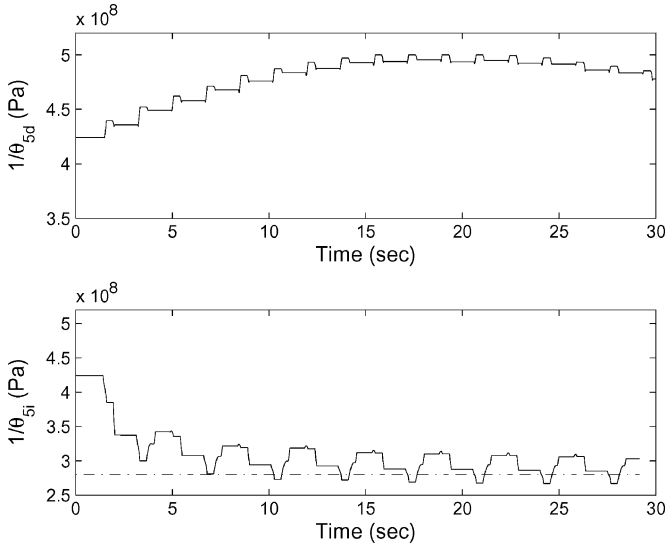

Fig. 8. Estimate of θ_5^{-1} with initial value $\widehat{\theta}_5^{-1}(0) = 4.2 \times 10^8$.

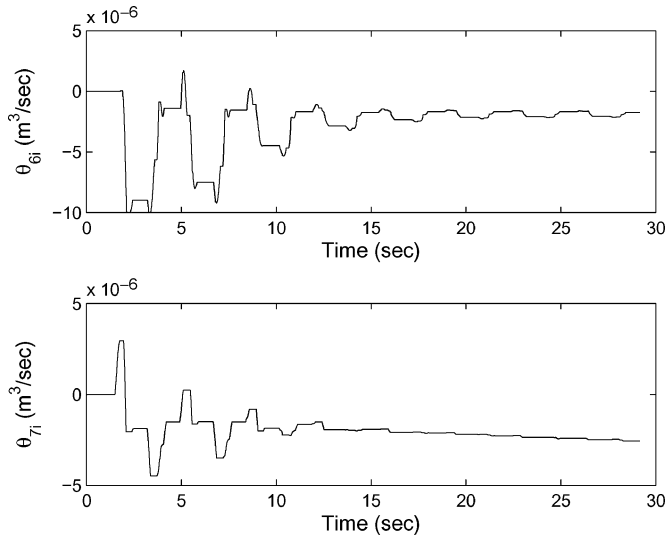

Fig. 9. Estimates of θ_6 ($\widehat{\theta}_6(0) = 0$) and θ_7 ($\widehat{\theta}_7(0) = 0$).

D. Comparative Experimental Results

In this experiment, the dSPACE controller sampling frequency was selected as $f_s = 1$ kHz. The following two controller algorithms were compared.

C1) The direct adaptive robust controller (DARC) in [9].

C2) The indirect adaptive robust controller (IARC) proposed in this paper.

To have a fair comparison, controller parameters of both the controllers are chosen to be the same when they have the same meaning. The lower and upper bound for $\theta_1 - \theta_7$ are set as $[60,\ 0,\ 0,\ 0,\ 2 \times 10^8,\ -10^{-5},\ -10^{-5}]$ and $[250,\ 100,\ 100,\ 100,\ 4 \times 10^8,\ 10^{-5},\ 10^{-5}]$, respectively. The initial values of the unknown parameters were kept same for both controllers. The desired trajectory shown in Fig. 3 has a maximum velocity $\omega_{\max} = 0.6$ rad/s and a maximum acceleration $\dot{\omega}_{\max} = 6$ rad/s^2.

Figs. 4–8 show the estimates for physical parameters θ_1, θ_2, θ_3, θ_4, and θ_5, respectively. In these figures, subscripts d and i are used for DARC and IARC algorithms respectively and the dashed line in the figure represents the offline estimates of the parameters. As seen from these figures, IARC has a much better convergence rate and final value accuracy of those parameters than DARC. The relatively more accurate parameter estimates of IARC may be used for other secondary purpose (e.g., system health monitoring). The accuracy of these physical parameter estimates with IARC design can also been seen from the estimate of the nominal value of lumped modeling uncertainties in the pressure channel (e.g., θ_6 and θ_7) shown in Fig. 9 and the tracking error in Fig. 10. As shown from these figures, as the physical parameter estimates of IARC approach their offline estimated values, smaller tracking errors exhibit at the end of the run and IARC achieves an even better steady-state tracking performance than DARC. The control inputs of DARC and IARC are shown in Fig. 11, which are comparable and reasonable.

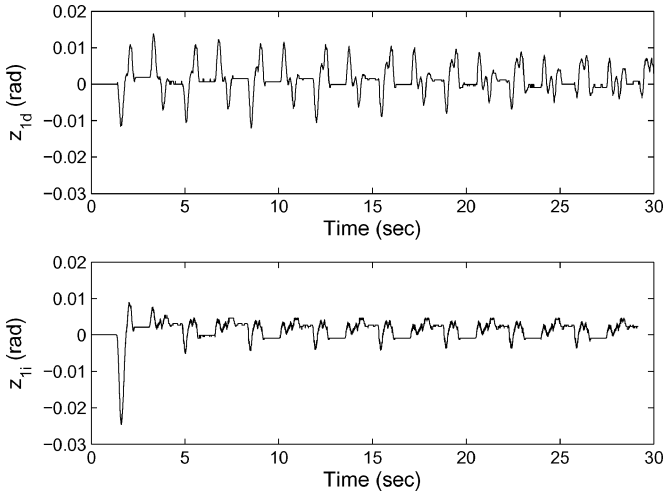

Fig. 10. Swing joint tracking error.

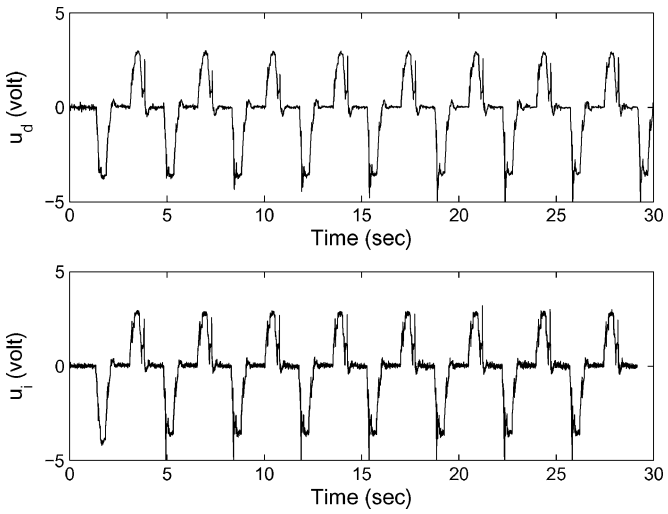

Fig. 11. Control input.

V. Conclusion

In this paper, an indirect adaptive robust controller is synthesized for precise motion control of electro-hydraulic systems

driven by single-rod hydraulic actuator. The proposed IARC focuses on accurate estimations of unknown parameters for secondary purposes such as health monitoring and fault detection as well. Comparative experiment results show that the proposed IARC controller achieves better parameter estimates and steady-state tracking accuracy than the previously developed DARC controller with comparable control effort.

REFERENCES

[1] P. M. FitzSimons and J. J. Palazzolo, "Part i: Modeling of a one-degree-of-freedom active hydraulic mount; part ii: Control," *ASME J. Dyn. Syst., Meas., Control*, vol. 118, no. 4, pp. 439–448, 1996.

[2] A. Alleyne and J. K. Hedrick, "Nonlinear adaptive control of active suspension," *IEEE Trans. Control Syst. Technol.*, vol. 3, no. 1, pp. 94–101, Jan. 1995.

[3] B. Yao, F. Bu, and G. T. C. Chiu, "Nonlinear adaptive robust control of electro-hydraulic servo systems with discontinuous projections," in *Proc. IEEE Conf. Dec. Control*, Tampa, FL, 1998, pp. 2265–2270.

[4] T. C. Tsao and M. Tomizuka, "Robust adaptive and repetitive digital control and application to hydraulic servo for noncircular machining," *Trans. ASME, J. Dyn. Syst., Meas., Control*, vol. 116, pp. 24–32, 1994.

[5] A. R. Plummer and N. D. Vaughan, "Robust adaptive control for hydraulic servosystems," *ASME J. Dyn. Syst., Meas. Control*, vol. 118, pp. 237–244, 1996.

[6] J. E. Bobrow and K. Lum, "Adaptive, high bandwidth control of a hydraulic actuator," *ASME J. Dyn. Syst., Meas., Control*, vol. 118, pp. 714–720, 1996.

[7] R. Vossoughi and M. Donath, "Dynamic feedback linearization for electro-hydraulically actuated control systems," *ASME J. Dyn. Syst., Meas., Control*, vol. 117, no. 4, pp. 468–477, 1995.

[8] A. Alleyne and R. Liu, "On the limitation of force tracking control for hydraulic servosystems," *ASME J. Dyn. Syst., Meas., Control*, vol. 121, no. 2, pp. 184–190, 1999.

[9] B. Yao, F. Bu, J. Reedy, and G. Chiu, "Adaptive robust control of single-rod hydraulic actuators: Theory and experiments," *IEEE/ASME Trans. Mechatronics*, vol. 5, no. 1, pp. 79–91, Feb. 2000.

[10] B. Yao and M. Tomizuka, "Adaptive robust control of MIMO nonlinear systems in semi-strict feedback forms," *Automatica*, vol. 37, no. 9, pp. 1305–1321, 2001.

[11] B. Yao, "High performance adaptive robust control of nonlinear systems: A general framework and new schemes," in *Proc. IEEE Conf. Dec. Control*, San Diego, CA, 1997, pp. 2489–2494.

[12] B. Yao and A. Palmer, "Indirect adaptive robust control of siso system in semi-strict feedback forms," in *Proc. 15th IFAC World Congr.*, Barcelona, Spain, 2002, pp. 1–6.

[13] H. E. Merritt, *Hydraulic Control Systems*. New York: Wiley, 1967.

[14] B. Yao and M. Tomizuka, "Smooth robust adaptive sliding mode control of robot manipulators with guaranteed transient performance," *Trans. ASME, J. Dyn. Syst., Meas. Control*, vol. 118, no. 4, pp. 764–775, 1996.

[15] S. Sastry and M. Bodson, *Adaptive Control: Stability, Convergence and Robustness*. Englewood Cliffs, NJ: Prentice-Hall, 1989, 07632.

[16] G. C. Goodwin and D. Q. Mayne, "A parameter estimation perspective of continuous time model reference adaptive control," *Automatica*, vol. 23, no. 1, pp. 57–70, 1987.

[17] M. Krstic, I. Kanellakopoulos, and P. V. Kokotovic, *Nonlinear and Adaptive Control Design*. New York: Wiley, 1995.

[18] B. Yao and M. Tomizuka, "Adaptive robust control of SISO nonlinear systems in a semi-strict feedback form," *Automatica*, vol. 33, no. 5, pp. 893–900, 1997.

[19] I. D. Landau, R. Lozano, and M. M'Saad, *Adaptive Control*. New York: Springer, 1998.

[20] B. Yao and M. Tomizuka, "Adaptive robust control of MIMO nonlinear systems in semi-strict feedback forms," in *Proc. IEEE Conf. Dec. Control*, 1995, pp. 2346–2351.

[21] B. Yao and M. Tomizuka, "Adaptive robust control of MIMO nonlinear systems in semi-strict feedback forms," in *Proc. IFAC World Congr.*, 1996, vol. F, pp. 335–340.

Amit Mohanty (S'10) received the B.Tech. degree in mechanical engineering from the Indian Institute of Technology, Kharagpur, India, in 2003, and the M.S. degree in mechanical engineering from Southern Illinois University, Carbondale, IL, in 2004. He is currently pursuing the Ph.D. degree in mechanical engineering from Ray W. Herrick Laboratories, Purdue University, West Lafayette, IN.

His research interests include adaptive and robust control of mechatronic systems, nonlinear observer design, fault detection, diagnostics, and adaptive fault-tolerant control.

Bin Yao (S'92–M'96–SM'09) received the B.Eng. degree in applied mechanics from Beijing University of Aeronautics and Astronautics, Beijing, China, in 1987, the M.Eng. degree in electrical engineering from Nanyang Technological University, Singapore, in 1992, and the Ph.D. degree in mechanical engineering from University of California at Berkeley, Berkeley, in 1996.

He has been with the School of Mechanical Engineering, Purdue University, West Lafayette, IN, since 1996 and promoted to the rank of Professor in 2007. He was honored as a Kuang-piu Professor in 2005 and a Chang Jiang Chair Professor in 2010 at the Zhejiang University, China as well.

Dr. Yao was a recipient of a Faculty Early Career Development (Career) Award from the National Science Foundation (NSF) in 1998 and a Joint Research Fund for Outstanding Overseas Chinese Young Scholars from the National Natural Science Foundation of China (NSFC) in 2005. He was the recipient of the O. Hugo Schuck Best Paper (Theory) Award from the American Automatic Control Council in 2004 and the Outstanding Young Investigator Award of ASME Dynamic Systems and Control Division (DSCD) in 2007. He has chaired numerous sessions and served in the International Program Committee of various IEEE, ASME, and IFAC conferences. From 2000 to 2002, he was the Chair of the Adaptive and Optimal Control Panel and, from 2001 to 2003, the Chair of the Fluid Control Panel of the ASME Dynamic Systems and Control Division (DSCD). He is currently the Chair of the ASME DSCD Mechatronics Technical Committee. He was a Technical Editor of the IEEE/ASME TRANSACTIONS ON MECHATRONICS from 2001 to 2005 and an Associate Editor of the *ASME Journal of Dynamic Systems, Measurement, and Control* from 2006 to 2009. More detailed information can be found at: https://engineering.purdue.edu/~byao.